Brain Structure and Function (2019) 224:759–777
https://doi.org/10.1007/s00429-018-1803-1

ORIGINAL ARTICLE

Cerebral resting state markers of biased perception in social anxiety

Benjamin Kreifelts[1] · Lena Weigel[1] · Thomas Ethofer[1,2] · Carolin Brück[1] · Michael Erb[2] · Dirk Wildgruber[1]

Received: 18 May 2018 / Accepted: 24 November 2018 / Published online: 1 December 2018

Abstract
Social anxiety (SA) comprises a multitude of persistent fears around the central element of dreaded negative evaluation and exclusion. This very common anxiety is spectrally distributed among the general population and associated with social perception biases deemed causal in its maintenance. Here, we investigated cerebral resting state markers linking SA and biased social perception. To this end, resting state functional connectivity (RSFC) was assessed as the neurobiological marker in a study population with greatly varying SA using fMRI in the first step of the experiment. One month later the impact of unattended laughter—exemplifying social threat—on a face rating task was evaluated as a measure of biased social perception. Applying a dimensional approach, SA-related cognitive biases tied to the valence, dominance and arousal of the threat signal and their underlying RSFC patterns among central nodes of the cerebral emotion, voice and face processing networks were identified. In particular, the connectivity patterns between the amygdalae and the right temporal voice area met all criteria for a cerebral mediation of the association between SA and the laughter valence-related interpretation bias. Thus, beyond this identification of non-state-dependent cerebral markers of biased perception in SA, this study highlights both a starting point and targets for future research on the causal relationships between cerebral connectivity patterns, SA and biased perception, potentially via neurofeedback methods.

Keywords Interpretation bias · Attention bias · Amygdala · Fusiform face area · Temporal voice area · Laughter

Introduction

Social anxiety (SA) represents a maladaptive mechanism presumably as old as the evolution to the establishment of a dominance-/submissiveness-based social hierarchy through nonverbal and later verbal cues rather than through physical violence or the threat thereof (Öhman 1986; Trower and Gilbert 1989). Accordingly, the fears in SA revolve around humiliation, exclusion and negative social evaluation in general.

SA exists in a wide spectrum of severity among the general population and its clinical form, termed social anxiety disorder (SAD), is one of the most common psychiatric disorders (Stein et al. 2010) associated with a profound loss of quality of life (Mendlowicz and Stein 2000) and great economic burden (Lipsitz and Schneier 2000). Neuropsychologically, SA is associated with cognitive biases thought to be causally linked to the maintenance of SA on the basis of psychological models (Clark and Wells 1995; Rapee and Heimberg 1997) and empirical data (Amir et al. 2009; Amir and Taylor 2012; Beard and Amir 2008). These biases are driven by a heightened sensitivity to social threat as exemplified by two of their most well-known forms, the negative interpretation and attention biases. The interpretation bias is characterized by a more negative evaluation of potential signals of social threat or a misinterpretation of ambiguous cues as socially threatening (Machado-de-Sousa et al. 2010; Quadflieg et al. 2007), whereas accelerated responses to social threat are representative of the attention bias (Gilboa-Schechtman et al. 1999; Mogg and Bradley 2002).

Commensurate with its clinical relevance, considerable effort has been made to elucidate the neural basis of SA.

Electronic supplementary material The online version of this article (https://doi.org/10.1007/s00429-018-1803-1) contains supplementary material, which is available to authorized users.

✉ Benjamin Kreifelts
benjamin.kreifelts@med.uni-tuebingen.de

[1] Department of Psychiatry and Psychotherapy, Eberhard Karls University of Tübingen, Calwerstr. 14, 72076 Tübingen, Germany

[2] Department of Biomedical Magnetic Resonance, Eberhard Karls University of Tübingen, Tübingen, Germany

While task-based neuroimaging studies primarily demonstrated increased cerebral responses to social threat in the limbic system, mediofrontal and orbitofrontal cortices as well as associative visual brain regions (reviewed in Brühl et al. 2014; Miskovic and Schmidt 2012), common findings from resting state functional connectivity (RSFC) studies indicate an association of SA with abnormalities in the connectivity patterns between the amygdala and frontal brain regions and within the so-called salience and default mode networks (reviewed in Kim and Yoon 2018). Evidence on the cerebral correlates of cognitive biases during social threat perception, in contrast, is relatively scarce. Studies in healthy participants (Browning et al. 2010) and SA (Kreifelts et al. 2014, 2017) consistently point to the lateral prefrontal cortex as pivotal cerebral structure in instantiating and modifying negative cognitive biases.

Importantly, consistent with the concept of SA as a persistent form of anxiety which exists also outside the context of social threat as a permanent disposition to exhibit biased cognition in SA-relevant situations, one might assume that this disposition should be represented at the neuronal level. However, to date, it remains unclear if such cerebral markers of negative cognitive biases in SA exist in the human brain outside the context of behavioral measurements in neuroimaging experiments.

Therefore, we designed a combined functional magnetic resonance imaging (fMRI) and behavioral study to investigate the existence of cerebral markers of negative cognitive biases in form of interpretation and attention biases in SA. To this end, we employed a novel, laughter-based behavioral design to assess biased social perception in a cohort of individuals exhibiting greatly varying levels of SA, ranging from completely socially non-anxious persons to individuals with severe forms of SA, and related the behavioral data to the results of a resting state neuroimaging study performed with the same cohort one month earlier. The time lag was introduced to ensure that observed cerebral markers did not solely reflect the individual emotional state at the time of bias assessment. RSFC patterns were investigated with regard to their correlation with SA severity, to which degree they predicted laughter-induced cognitive biases during social perception and with regard to their potential mediation of the relationship between SA and biased perception.

In the behavioral experiment, audiovisual portrayals of laughter varying along the emotional dimensions of valence, arousal and dominance were presented in an unattended fashion during a task where the participants rated the valence of shortly presented faces. This design aimed at evaluating the effects of laughter valence, arousal, and dominance on face ratings and response times as behavioral correlates of cognitive biases. Critically, while the faces were strictly neutral, the participants were informed before the experiment that there might be minimal emotional expressions in the face stimuli. Laughter-induced biases were calculated separately for the impact of the valence-, arousal- and dominance component of unattended laughter stimuli on face ratings (i.e., interpretation bias) and response times (i.e., attention bias). Distorted laughter (i.e., non-social) stimuli were employed to additionally assess general effects of laughter on face ratings.

But why use laughter? The employment of laughter in SA research draws upon recent empirical findings and evolutionary as well as ecological considerations: The fear of being laughed at is not only a characteristic symptom of SA (Havranek et al. 2017), but it could also be shown that SA is associated with laughter induced interpretation and attention biases (Kreifelts et al. 2014, 2017; Ritter et al. 2015). From an evolutionary perspective, laughter is an ancient vocal means of social communication (Davila Ross et al. 2009) and represents one of the earliest signals to communicate group bonding (Provine 2013) as well as social exclusion (Eibl-Eibesfeldt 1970). Correspondingly, laughter communicates the emotional state of the laugher not only in terms of valence and arousal but also in terms of dominance (Szameitat et al. 2009) which again dovetails with the conceptualization of SA as an maladaptive phenomenon in an evolutionary dominance/submissiveness system (Öhman 1986; Trower and Gilbert 1989). Finally, as a very frequent and inherently dynamic and multimodal communication signal, laughter has a high ecological validity as vector of social threat. The unattended laughter processing design of our behavioral experiment was selected to further increase ecological validity as, under natural circumstances, laughter is rarely explicitly evaluated but commonly perceived in an implicit way.

The RSFC analyses focused primarily on the amygdala as one central structure of the emotion-processing system as well as key regions of the social perception system [i.e., the fusiform face area (FFA; Kanwisher et al. 1997), the temporal voice area (TVA; Belin et al. 2000) and the audiovisual integration area for nonverbal signals from voice and face in the posterior superior temporal sulcus (pSTS), here termed temporal voice–face integration area (TVFIA); Kreifelts et al. 2007, 2009] which are characterized by their preferential processing of the most common carrier signals of social threat (i.e., voices and faces) in human face-to-face communication. The latter three were determined applying separate functional fMRI localizer experiments.

At the behavioral level, we expected that threat-relevant information of contextual unattended laughter (i.e., negative valence, high arousal and high dominance) would be attributed to the ambiguous face stimuli and systematically reflected in the responses to these. Thus, we expected the following SA-related laughter-induced cognitive biases:

SA correlates with

(a) increasingly negative face ratings and faster responses in the context of negative valence laughter.
(b) increasingly faster responses in the context of high arousal laughter.
(c) increasingly negative face ratings and faster responses in the context of high dominance laughter.

The RSFC analysis was performed without specific hypotheses due to the lack of directly comparable studies reported in the literature and divergent results for the association of SA and amygdala RSFC patterns in previous studies (Kim and Yoon 2018) with one exception: regarding numerous studies indicating an involvement of the amygdala in the RSFC representation of SA (Kim and Yoon 2018), we hypothesized this finding to be replicated in our study in form of a linear association between SA and the RSFC patterns of the amygdala.

Materials and methods

Participants

28 individuals (14 male, mean age 24.8 years, SD 4.0 years, range 19–39 years) were recruited by inviting volunteers who perceived themselves as either very socially anxious or very outgoing through public announcements. All participants were examined using the Structured Clinical Interview for DSM-IV (SCID; Wittchen et al. 1997) before inclusion into the study. Additionally, the Liebowitz Social Anxiety Scale (LSAS; German self-report version, Stangier and Heidenreich 2003) was applied to assess the severity of SA. Thirteen participants fulfilled the DSM-IV clinical criteria of SAD while the remaining participants exhibited varying levels of SA below the clinical threshold. Three participants (two of them with SAD) were diagnosed with a minor depression while the remaining participants did not suffer from any psychiatric disorder. Three of the participants with SAD had a history of major depression and all of these had been in remission for more than six months before study inclusion. None of the participants was taking any regular medication, or had a history of substance abuse, or neurological illness. General anxiety and depressive symptoms were evaluated applying the State-Trait-Anxiety-Inventory (STAI, German version; Laux et al. 1981) and the Beck Depression Inventory (BDI-II, German version; Hautzinger 1991), respectively. Verbal intelligence was determined with the "Mehrfachwahl-Wortschatz-Intelligenz-Test" (MWT-B; Lehrl 2005). All participants were right-handed as evaluated with the Edinburgh Inventory (Oldfield 1971), native German speakers, and reported normal hearing and normal or corrected to normal visual acuity. 26 of the 28 participants reported here were also included in another experiment on laughter perception (Kreifelts et al. 2017). The full experimental protocol of the overarching research project is detailed in the Supplementary material.

The socio-demographic and psychometric data of the study sample are given in Table 1. For their participation, the participants received a monetary expense allowance.

Compliance with ethical standards

The study was approved by the Ethics Committee of the University of Tübingen and performed in accordance with the Code of Ethics of the World Medical Association (Declaration of Helsinki, 1964) and its later amendments. Before their inclusion into the study, all participants gave written informed consent.

This work was supported by grants of the Fortüne-Program of the University of Tübingen (fortüne 1997-0-0, and fortüne 2140-0-0). The authors declare that they have no conflict of interest.

Stimulus material

The stimulus material consisted of neutral face pictures as target stimuli and videos portraying laughing faces as unattended contextual stimuli.

The 20 neutral face stimuli (mean valence rating on a self-assessment manikin (SAM) scale ranging from 1 (very negative) to 9 (very positive): 4.96; SD 0.22; range 4.6–5.4) were pictures taken from video sequences of professional actors (3 female, 3 male), were balanced for the gender of the depicted face and had been evaluated in a prestudy (see Supplementary material), and were selected to portray a strictly neutral expression.

Table 1 Socio-demographic and psychometric data

	Mean (SD)
LSAS	42.6 (27.9)
SAD	13/28
STAI-X1	38.4 (8.7)
STAI-X2	40.3 (12.1)
BDI	7.2 (5.7)
Gender	14 f, 14 m
Age	24.8 (4.0)
IQ (MWT-B)	115.8 (11.3)

LSAS Liebowitz Social Anxiety Scale, *SAD* social anxiety disorder, *STAI* State Trait Anxiety Inventory, *BDI* Beck Depression Inventory, *MWT-B* "Mehrfachwahl-Wortschatz-Intelligenz-Test", a short test of verbal intelligence

The 60 laughter sequences (duration 1.5 s) had been recorded from eight professional actors and selected to display a broad spectrum of socio-emotional information (see Fig. 1) with regard to the emotional dimensions of valence [mean 5.44; SD 1.3 on a SAM scale ranging from 1 (very negative) to 9 (very positive)], arousal [mean 5.46; SD 1.7 on a SAM scale ranging from 1 (very calm) to 9 (highly aroused)] and dominance [mean 5.15; SD 1.0 on a SAM scale ranging from 1 (very submissive) to 9 (very dominant)] as evaluated in three prestudies by healthy individuals (valence: $n=14$, 7 female, mean age 24.6 years, SD 3.3 years; arousal: $n=14$, 8 female, mean age 23.4 years, SD 2.1 years; dominance: $n=14$, 7 female, mean age 24.3 years, SD 3.5 years). For further details on these three prestudies, see the Supplementary material. The broad spectrum in emotional information across the three dimensions was achieved by selecting equal numbers of exemplars ($n=20$) of taunting, joyful and tickling laughter as it has been demonstrated that each of the three dimensions explains a considerable amount of unique variance across these laughter types (Szameitat et al. 2009). The stimulus set was balanced for the gender of the actors (33 female, 27 male). Further details on stimulus production and selection are reported elsewhere (Kreifelts et al. 2014). In the present stimulus set, the three-dimensional parameters exhibited the following inter-relations: valence was positively correlated with arousal ($r=0.34$) and negatively correlated with dominance ($r=-0.56$) while dominance was positively correlated with arousal ($r=0.34$).

The 60 laughter stimuli were complemented by 20 (6 taunting, 8 tickling, 6 joyful; 10 female, 10 male) laughter stimuli manipulated with the aim to remove all social information as baseline non-social stimulus type. This was done by applying Adobe Premiere Pro's "twirl" effect which preserves movement, luminance and coloring but effectively renders any facial features completely unrecognizable to the visual stimulus component and an algorithm based on a Fourier transform to the laughter sounds. This algorithm (Werner and Noppeney 2010) preserves basic acoustic features (e.g. basic frequency, variability of volume, harmonic structure) but makes the sounds unrecognizable as either "vocal" or "laughter".

Experimental design

The stimulus material was presented on an LG Flatron L1953PM 17-inch flat screen with a resolution of 800 × 600 pixels while the participant was sitting in a comfortable position about 70 cm from the screen. Each of the overall 80 trials (for an example see Fig. 2) began with the presentation of a neutral face image (duration 150 ms). This stimulus was immediately followed by a laughter stimulus. It was the participants' task to perform a rating of the face stimuli on a three-point scale (i.e., positive, neutral, or negative) as fast as possible and to disregard the audiovisual laughter/non-social stimuli. The response window was 3 s from the face stimulus onset. The laughter video was followed by a response scale. Responses were given on a computer keyboard. The horizontal orientation of the response scale was balanced across the participants to avoid any potential laterality effects. The order of stimulus presentation was randomized. Face ratings and response times were recorded as outcome parameters. The software presentation (Neurobehavioral Systems Inc., Berkeley, CA, USA) was used for the stimulus presentation and the recording of the participants' responses. The participants were informed that positive/negative expressions among the face stimuli might be minimal.

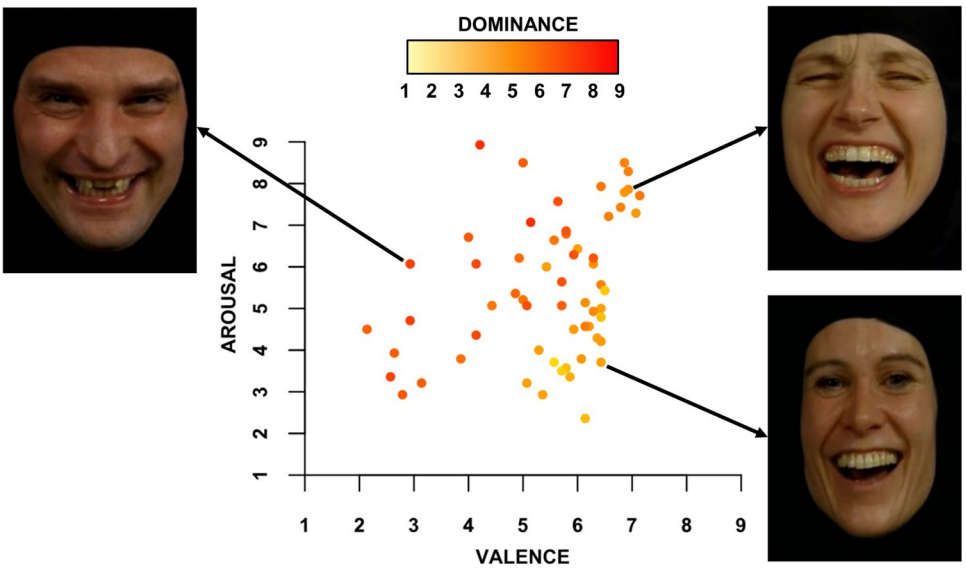

Fig. 1 Emotional characterization of the laughter stimuli. The employed laughter sequences are displayed in a three-dimensional continuum with the dimensions valence, arousal and dominance. While valence and arousal are depicted on the *x*- and *y*-axes of the scatter plot, the third dimension dominance is represented in form of a color code. Additionally, it is shown where typical exemplars of taunting (left upper corner), tickle (right upper corner) and joyful (right lower corner) are located in the valence-arousal-dominance continuum

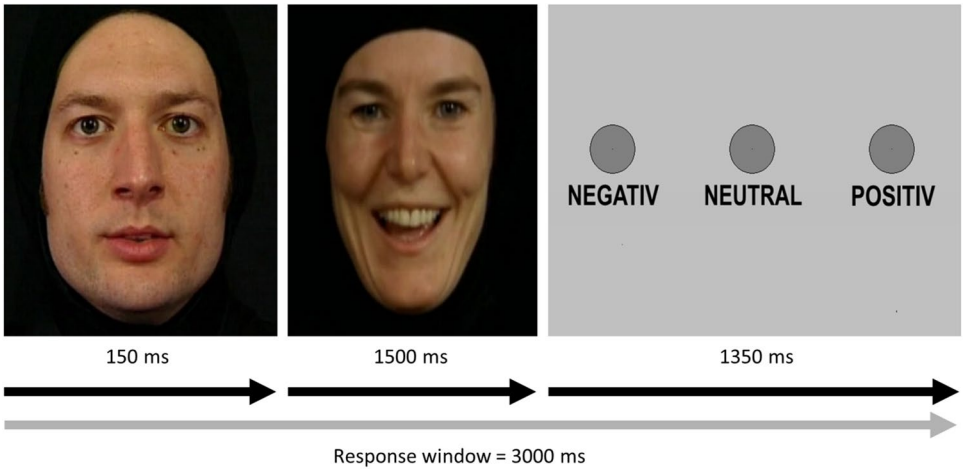

Fig. 2 Trial design. A neutral face was displayed for 150 ms followed by a 1.5-s laughter sequence or a non-social control stimulus and then a rating scale. It was the participants' task to rate the valence of the face (negative, neutral, positive) disregarding the audiovisual laughter/non-social stimulus within a response window of 3 s from the face stimulus onset

Resting state fMRI measurements and functional localizer experiments

For the resting state measurements (duration: about 7 min and 15 s), the participants were instructed to keep their eyes closed with no further task while they waited for the "calibration measurements" to finish.

Then, three fMRI experiments were performed to localize the voice-sensitive TVA (Pernet et al. 2015; Belin et al. 2000), the face-sensitive FFA (Kanwisher et al. 1997) and the TVFIA in the pSTS (e.g., Ethofer et al. 2013; Kreifelts et al. 2007, 2009, 2010).

The voice localizer experiment was developed based on the study by Belin et al. (2000) in form of a block design experiment with 24 stimulation blocks and 12 silent periods (each 8 s) with a passive-listening task. The stimulus material comprised 12 blocks of human vocal sounds (speech, sighs, laughs, cries), 6 blocks of animal sounds (e.g., gallops, various cries) and 6 blocks of environmental sounds (e.g., cars, planes, doors, telephones). For the face localizer, pictures from four different categories (faces, houses, objects, and natural scenes) were employed within a block design. The experimental design has been adapted from previous studies on face processing (Epstein et al. 1999; Kanwisher et al. 1997). Each category and block (duration 16 s) contained 20 stimuli. Eight blocks of each category pseudorandomized within the experiment were shown. Constant attention was ascertained with a one-back task. The participants had to press a button on a fiber optic system (LumiTouch, Photon Control, Burnaby, Canada) when a picture was directly repeated. Visual stimuli were back-projected onto a screen placed in the magnet bore behind the participant's head and viewed by the participant through a mirror system mounted onto the head coil.

The stimulus material of the voice–face integration localizer consisted of video portrayals (1.6 s) of 60 words spoken by six professional actors with an emotional (i.e., angry, disgusted, alluring, fearful, happy, or sad) or neutral speech melody and congruent facial expression. All stimuli were presented under three conditions: auditory (A), visual (V), and audiovisual (AV) with a total of 180 stimuli per participant. Auditory stimuli were presented through MR compatible headphones (MR confon GmbH, Magdeburg, Germany). Within a block design, the stimuli were divided into 12 blocks (A, V, and AV) with five stimuli each. The participants' task was to identify the second "male" stimulus within each block to ensure constant attention to the stimuli. Responses were given by pressing a button on the fiber optic system (see above) with their right index finger.

All three experimental designs have been validated in previous studies (voice and face localizers: Ethofer et al. 2013; Kreifelts et al. 2009, 2010, 2013; audiovisual integration localizer). Further details on the stimulus material and experimental designs have been reported elsewhere (Kreifelts et al. 2010).

The fMRI data were acquired approximately one month (30.9 days, SD 3.6, range 21–42 days) before the behavioral data.

Image acquisition

Functional images (echo-planar imaging sequence, repetition time (TR) = 1.7 s, echo time (TE) = 30 ms, voxel size: $3 \times 3 \times 5$ mm^3, 30 axial slices with acquisition in interleaved descending order and a slice thickness of 4 mm + 1 mm gap, oriented along the anterior commissure–posterior commissure plane) were recorded with a 3-T scanner (Siemens PRISMA, Erlangen, Germany). For each participant, 250 whole-brain functional MRI images were recorded in the resting state, 232 images for voice localizer, 368 images for the face localizer and 239 images for the voice–face integration localizer. Additionally, T1-weighted anatomical images (TR = 2300 ms, TE = 4.18 ms, time to inversion (TI) = 900 ms, voxel size $1 \times 1 \times 1$ mm^3) and a field

map for correction of image distortions (TR = 400 ms, TE(1) = 4.92 ms, TE(2) = 7.38 ms, voxel size 3 × 3 × 4 mm^3, 36 slices, slice thickness 3 mm + 1 mm gap) were acquired.

Analysis of study population data and behavioral data

IBM SPSS Statistics Version 21 (IBM Corporation, Armonk, NY, USA) was used for the statistical analyses. Face ratings were transformed to numerical values (1 = negative; 2 = neutral; 3 = positive). For the analysis of the response time data, any responses outside two standard deviations from the individual mean response time were excluded from the analysis to prevent biases in the response time data through outliers. The individual effects of laughter valence, arousal and dominance on the face ratings were calculated as the coefficient of the regression of the separate stimulus characteristics (i.e., laughter valence etc.) on the outcome parameters (i.e., face ratings and response times).

The Kolmogorov–Smirnov test was applied to verify the normal distribution of the population parameters and behavioral data. Bivariate correlation analyses were employed to investigate associations of SA (LSAS) with other population parameters (age, gender, BDI-II, STAI-X1/X2, MWT-B) as well as with the individual influences of laughter valence, arousal and dominance on face ratings and response times.

Additionally, it was tested if laughter generally differed from non-social stimuli with regard to the effect on the face ratings or response times (paired *t* tests), if individual SA was generally associated with face ratings or response times, either in the context of laughter or of non-social stimuli, or the contrast of these conditions, and if there were overall effects of laughter valence, dominance and arousal on face ratings irrespective of individual SA (one sample *t* tests). Two-tailed *p* values are given for all analyses where no a priori directional hypotheses existed.

Analysis of imaging data

Statistical parametric mapping software (SPM8; http://www.fil.ion.ucl.ac.uk/spm) was used to analyze the imaging data. The first five EPI images from each run were removed to exclude measurements preceding T1 equilibrium.

Localizer experiments

For the localizer experiments, the preprocessing comprised realignment, unwarping using a static field map, coregistration of anatomical and functional images, segmentation of the anatomical images, normalization into MNI space (Montreal Neurological Institute) with a resampled voxel size of 3 × 3 × 3 mm^3, temporal smoothing with a high-pass filter (cutoff frequency of 1/128 Hz) and spatial smoothing employing a Gaussian kernel (8 mm full width at half maximum).

The responses to the single categories (faces (F), houses (H), objects (O), and natural of scenes (S) in the face localizer; voices (V), animal sounds (A), and environmental sounds (E) in the voice localizer and auditory stimuli (A), visual stimuli (V) and audiovisual stimuli (AV) in the voice–face integration localizer) were separately modeled with a box-car function corresponding to the block duration (16 s in the face localizer and 8 s in the voice localizer and the voice–face integration localizer) convolved with the HRF. Data from the individual first-level general linear models were employed to create contrast images [face sensitivity: F > H, O, S; voice sensitivity: V > A, E; voice–face integration: AV > max(A, V)] for each subject which were then submitted to a second-level random-effect analysis.

Definition of anatomical and functional regions of interest

The bilateral amygdalae were defined as anatomical ROIs using the automatic anatomic labeling (AAL) toolbox (Tzourio-Mazoyer et al. 2002). Group-level significance of localizer activation was assessed using FWE correction with $p < 0.05$ at cluster level and a voxel-wise threshold of $p < 0.001$ within a priori defined anatomical ROIs (voice localizer: temporal lobe, face localizer: fusiform gyrus, voice–face integration localizer: superior and middle temporal gyri), i.e., applying small volume correction (Worsley et al. 1996) for the respective anatomical ROIs. To avoid confounds due to varying sizes of the anatomical and functional ROIs, a size of 81 voxels corresponding to the mean volume of the anatomical amygdala ROIs was defined for all three types of functional ROIs. Thus, the TVA was defined as the 81 most voice-sensitive voxels within the most voice-sensitive cluster in the respective temporal lobe, the FFA as the 81 most face-sensitive voxels within the most face-sensitive cluster in respective fusiform gyrus and the TVFIA as the 81 most AV-sensitive adjoining voxels within the respective superior and middle temporal gyri. The voice and face sensitivity of all ROIs was further explored applying conservative criteria implying preferentiality for voices or/and faces [i.e., minimum difference criteria: V > max(A, E) and F > max(H, O, S)].

Resting state functional connectivity analysis

The RSFC analyses were performed using the CONN toolbox (v16b; Whitfield-Gabrieli and Nieto-Castanon 2012) implemented in SPM8. The spatial preprocessing included the same sequence of steps as for the localizer experiments. With regard to the temporal processing, the participants' movement parameters, their first order derivatives and the BOLD signal from white matter and cerebrospinal

fluid (each with five temporal components) were entered into the analysis as covariates to minimize confounding influences from these factors. The residual BOLD time series was then band-pass filtered (0.008–0.9 Hz). In the individual first-level analyses, bivariate correlation coefficients were calculated as linear measures of functional connectivity for the ensuing analyses. These were Z transformed for the group-level analyses.

The primary analyses were ROI-to-ROI analyses between the ROIs as defined above. Here, the individual between-ROI connectivity estimates were correlated at the group level with those behavioral effects of laughter on face ratings which exhibited an association with SA severity (e.g., the effect of laughter valence) as well as with SA severity itself. Statistical inference was based on random effects analyses. Associations between behavioral parameters/SA severity and ROI-to-ROI connectivity are reported at $p < 0.05$, two-tailed, applying false discovery rate (FDR) correction with regard to the number of between-ROI connections.

The ROI-to-ROI analyses were complemented with exploratory ROI-to-voxel analyses to detect associations between behavioral parameters/SA severity and the RSFC of the ROIs also with other brain regions. Here, the significance of observed connectivity patterns was assessed using FDR correction at cluster level ($p < 0.05$) in combination with a voxel-wise threshold of $p < 0.005$, uncorrected. Additionally, the results were Bonferroni corrected for the number of seed ROIs and the direction of the association of functional connectivity and the behavioral parameters/SA severity. Thus, only clusters reaching a threshold of $p < 0.0036$, FDR corrected at cluster level, were deemed significant.

Mediation analysis

For RS connections where SA, one of the perception biases and FC were significantly intercorrelated, a potential mediation of the effect of SA on the perception bias through the RSFC pattern was tested employing a bootstrapping approach (Preacher and Hayes 2008) which is robust against potential deviations of the data from a normal distribution and which affords the assessment of multiple mediation effects and the inclusion of covariates. For details, see the Supplementary material. In case of multiple potentially mediating RS connections, total, separate and differential mediation effects were investigated. Observed mediation effects were tested for their specificity using post hoc mediation analyses where state (STAI-X1) and trait (STAI-X2) anxiety as well as depressive symptoms (BDI) were included as covariates.

Results

Population characteristics

The participants exhibited a broad spectrum of SA severity. For an overview of the psychometric and socio-demographic characteristics of the study sample see Table 1. With the exception of gender, all population parameters were normally distributed (all $Z < 1.0$, all $p > 0.05$). SA (i.e., LSAS) was significantly correlated with general state (STAI-X1, $r = 0.67$, $p < 0.001$) and trait anxiety (STAI-X2, $r = 0.69$, $p < 0.001$) as well as depressive symptoms (BDI, $r = 0.64$, $p < 0.001$) while there was no significant correlation with any of the other population parameters (all abs(r) < 0.35, all $p > 0.05$).

Face ratings and response times

All measures of face ratings and response times were normally distributed (all $Z < 1$, all $p > 0.05$). Three types of response biases associated with SA were observed for the effects of laughter valence, dominance and arousal:

Laughter valence-related interpretation bias (V-IB)

SA was positively correlated with the effect of laughter valence on face ratings ($r = 0.39$, $p = 0.02$, one-tailed; see Fig. 3a, top panel). This effect is driven by more negative face ratings in the context of negative valence laughter as exemplified in individuals with high SA (i.e., SAD; see Fig. 3a, bottom panel).

Laughter dominance-related interpretation bias (D-IB)

In contrast, SA was negatively correlated with the effect of laughter dominance on face ratings ($r = -0.57$, $p < 0.001$, one-tailed; see Fig. 3b, top panel). This effect can be visualized by the more negative face ratings in the context of high dominance laughter as exemplified in individuals with high SA (i.e., SAD) while in individuals with lower social anxiety there is a tendency towards more positive face ratings in the context of high dominance laughter (see Fig. 3b, bottom panel).

Laughter arousal-related attention bias (A-AB)

The effect of laughter arousal on response times was also negatively correlated with SA ($r = -0.46$, $p = 0.006$, one-tailed; see Fig. 3c, top panel). This effect is driven by faster response times to faces in the context of high arousal

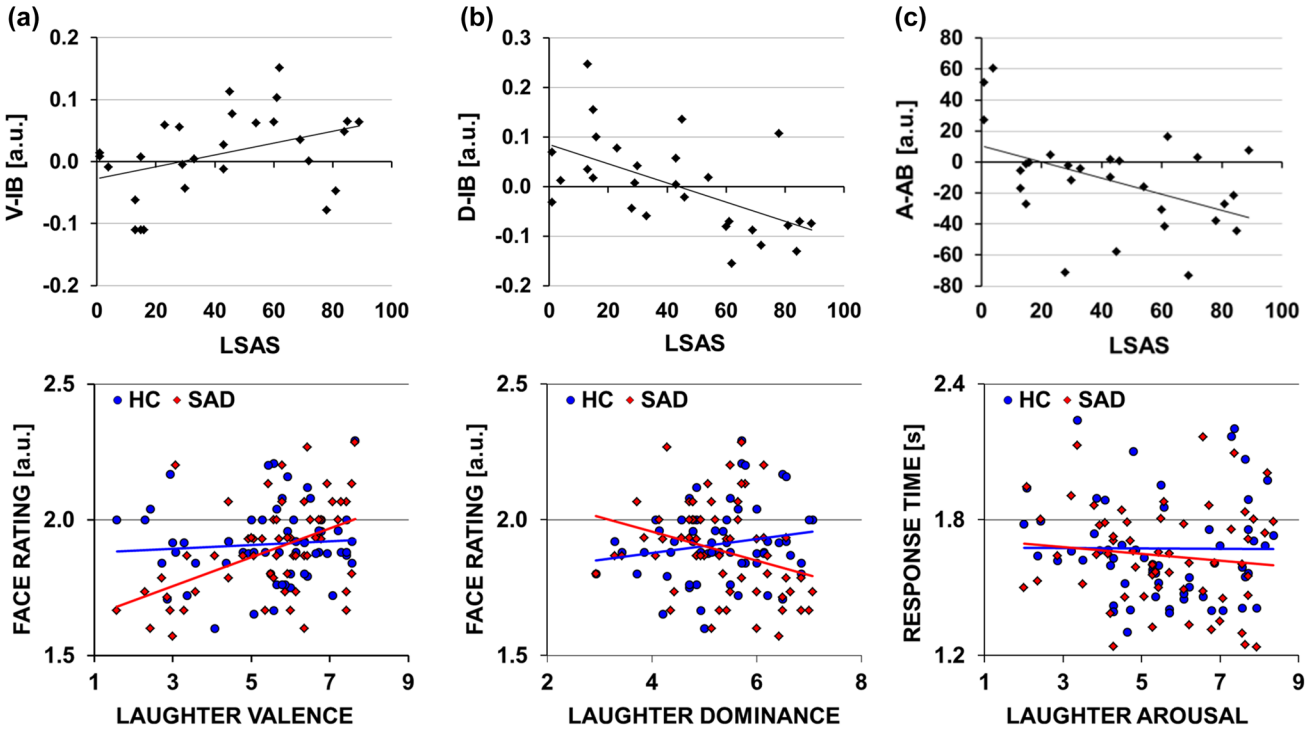

Fig. 3 SA-associated cognitive biases during laughter perception. The panels in the top row show the laughter-induced valence-related interpretation bias (V-IB) (**a**), dominance-related interpretation bias (D-IB) (**b**) and arousal-related attention bias (A-AB) (**c**) in their association with SA. The coefficients (in a.u.) from the within-subject regression of face ratings (**a, b**) or response times (**c**) on the valence (**a**), dominance (**b**) and arousal (**c**) of the laughter stimuli are plotted against the individual LSAS scores. The panels in the bottom row further illustrate the way in which SA influences the effects of the emotional properties of the laughter stimuli on the processing of the neutral face target stimuli. To this aim, the average stimulus-wise face ratings (**a, b**) and response times (**c**) are plotted against the valence (**a**), dominance (**b**) and arousal (**c**) of the ensuing laughter stimuli separately for healthy participants (HC) and participants with a diagnosis of SAD

laughter as exemplified in individuals with high SA (i.e., SAD) (see Fig. 3c, bottom panel).

Otherwise, there were no significant associations between laughter valence, dominance or arousal and SA regarding face ratings or response times (all abs(r) < 0.15, all p > 0.46). Overall, face ratings and response times were not significantly different in the context of laughter [mean individual face ratings: 1.89 (SD 0.22), mean individual response times: 1523 ms (SD 472 ms)] as compared to the non-social stimuli (mean individual face ratings: 1.88 (SD 0.27), mean individual response times: 1496 ms (SD 479 ms); both $t(27) > 0.8$, both $p > 0.42$). Neither face ratings nor response times were associated with SA in the general context of laughter (both abs(r) < 0.01; both $p > 0.95$) or non-social stimuli (both abs(r) < 0.11, both $p > 0.57$), nor for the contrast of these conditions (i.e., laughter vs. non-social stimuli; both abs(r) < 0.16, both $p > 0.22$).

ROI characteristics

The ROI characteristics are graphically displayed in Fig. 4. The bilateral TVA were highly voice sensitive with strong preferentiality for voices (right: sensitivity: $t(27) = 12.4$, $p < 0.001$; preferentiality: $t(27) = 9.8$, $p < 0.001$; left: sensitivity: $t(27) = 12.2$, $p < 0.001$; preferentiality: $t(27) = 9.9$, $p < 0.001$; Fig. 4, red areas). The right FFA exhibited both a face-sensitive and a face-preferential response (sensitivity: $t(27) = 5.6$, $p < 0.001$; preferentiality: $t(27) = 2.1$, $p = 0.02$; Fig. 4, right green area), whereas the left FFA was not found to be face preferential when applying the minimum difference criterion (i.e., F − max(H, O, S)), while showing face-sensitive responses (sensitivity: $t(27) = 5.0$, $p < 0.001$; preferentiality: $t(27) = 0.8$, $p > 0.05$; Fig. 4, left green area). The right TVFIA exhibited an audiovisual integration effect ($t(27) = 3.2$, $p = 0.002$; Fig. 4, blue area), while no TVFIA with a significant audiovisual integration effect (i.e., mean contrast estimates for the audiovisual integration effect [AV − max(A, V)] from 81 adjacent voxels not above the significance level of $p < 0.05$) was observed in the left pSTS. Additionally, the right TVFIA was voice sensitive and preferential (sensitivity: $t(27) = 6.0$, $p < 0.001$; preferentiality: $t(27) = 3.9$, $p < 0.001$). Towards faces it exhibited sensitivity but only a trend towards a preferential response (sensitivity: $t(27) = 5.1$, $p < 0.001$; preferentiality:

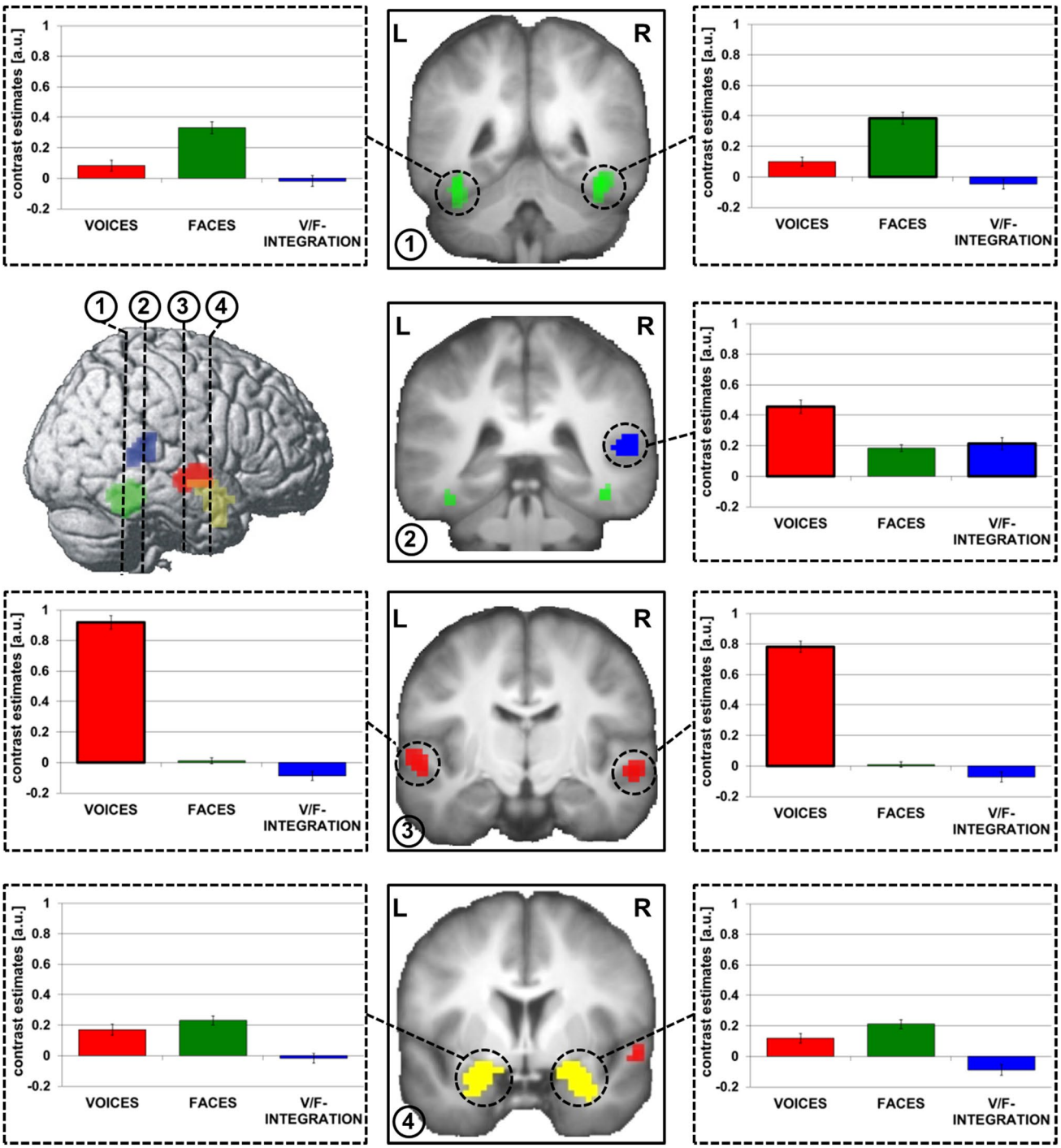

Fig. 4 Voice and face processing areas. The bilateral FFA (green), the bilateral TVA (red), the right TVFIA (blue) and the bilateral amygdala (yellow) are shown rendered onto the lateral view of a standard brain and coronal slices of the sample's mean anatomical image. The panels show the functional characteristics of these ROI, i.e., their response sensitivity for voices, faces and stronger responses to bimodal dynamic voice/face presentations as compared to voices or faces alone. Bold frames indicate that the conservative minimum difference contrast criterion for preferential responses to voices or faces or for voice–face integration was met (for details see "Definition of anatomical and functional regions of interest" in "Materials and methods")

$t(27) = 1.6$, $p = 0.06$). The amygdalae were found to be voice and face sensitive while not displaying strictly preferential responses for these cues (right: voices: sensitivity: $t(27) = 2.2$, $p = 0.02$; preferentiality: $t(27) = -1.4$, $p > 0.05$; faces: sensitivity: $t(27) = 4.3$, $p = < 0.001$; preferentiality: $t(27) = 1.4$, $p > 0.05$; left: voices: sensitivity: $t(27) = 2.7$,

$p = 0.006$; preferentiality: $t(27) = 0.1$, $p > 0.05$; faces: sensitivity: $t(27) = 4.4$, $p = < 0.001$; preferentiality: $t(27) = 0.4$, $p > 0.05$).

Resting state correlates of SA

In the ROI analysis, SA was significantly and positively correlated with the RSFC between the left and the right amygdala ($t(26) = 3.4$, $p(\text{FDR}) = 0.01$), between the left amygdala and the right TVA ($t(26) = 2.6$, $p(\text{FDR}) = 0.04$), and between the left and the right TVA ($t(26) = 2.8$, $p(\text{FDR}) = 0.03$; see Fig. 5).

At the whole brain level, the right FFA seed RSFC with two areas in the visual primary and association cortex exhibited a positive correlation with SA and the RSFC between the left FFA and the supplementary and right premotor cortex was likewise associated with SA. For the right TVA seed, the seed to voxel analysis confirmed the positive correlation of its RSFC with the left TVA within a larger cluster encompassing parts of the left middle and superior temporal gyri, temporal pole and left Rolandic operculum and SA (see Table 2).

Resting state correlates of laughter valence-, dominance- and arousal-related cognitive biases

Laughter valence-related interpretation bias (V-IB)

In the ROI analysis, the V-IB was positively associated with the RSFC between the left and the right amygdala ($t(26) = 2.5$, $p(\text{FDR}) = 0.047$), and between the left amygdala and the right TVA ($t(26) = 2.6$, $p(\text{FDR}) = 0.047$). Additionally, the V-IB correlated with the RSFC between the right TVFIA and left amygdala ($t(26) = 2.4$, $p(\text{FDR}) = 0.047$), the left TVA ($t(26) = 2.4$, $p(\text{FDR}) = 0.047$) and the right ($t(26) = 2.3$, $p(\text{FDR}) = 0.047$) and left FFA ($t(26) = 2.6$, $p(\text{FDR}) = 0.047$; see Fig. 5a).

Outside the RS connections between the predefined ROI, a positive correlation of the V-IB and the RSFC between the left amygdala and the left visual association cortex of the inferior temporal cortex anterior to the left FFA was observed (see Table 3).

Laughter dominance-related interpretation bias (D-IB)

The ROI analysis revealed that the D-IB was negatively correlated with the RSFC between the right amygdala and the left FFA ($t(26) = -3.3$, $p(\text{FDR}) = 0.009$), the left and the right FFA ($t(26) = -3.5$, $p(\text{FDR}) = 0.009$), the right FFA and the right TVFIA ($t(26) = -3.0$, $p(\text{FDR}) = 0.02$), and between the right TVFIA and the left TVA ($t(26) = -3.2$, $p(\text{FDR}) = 0.02$; see Fig. 5b).

At the whole brain level, additional significant negative correlations of the D-IB and the RSFC between the right TVFIA and two other brain regions, one in the bilateral medial visual association cortex centered on the lingual gyri and the other in the temporo-occipital junction adjacent to the two posterior ascending branches of the STS were detected (see Table 4).

Laughter arousal-related attention bias (A-AB)

In the ROI analysis, the A-AB exhibited a negative linear relationship with the RSFC between the right amygdala and the right FFA ($t(26) = -2.8$, $p(\text{FDR}) = 0.03$) as well as between the right FFA and the bilateral TVA (left: $t(26) = -2.4$, $p(\text{FDR}) = 0.04$; right: $t(26) = -2.9$, $p(\text{FDR}) = 0.03$; see Fig. 5c).

At the whole brain level, both negative and positive correlations between the A-AB and RSFC patterns were observed. While negative correlations were found for the RS connections between the left FFA and the area in the more anterior fusiform gyrus extending well into the bilateral inferomedial visual association cortex and the cerebellum, between the right TVFIA and the posterior cingulate cortex (PCC)/precuneus and between the left amygdala and a larger midline area centered on the bilateral supplementary motor area (SMA) and the bilateral paracentral lobule (see Table 5).

Mediation analyses

The mediation analysis revealed that the RSFC patterns between the left amygdala and the right amygdala (M_1) and between the left amygdala and the right TVA (M_2) formally fully mediated the influence of SA (X) on the V-IB (Y; see Table 6). Additional analyses demonstrated that the mediation effect (ab_{TOTAL}) remained significant when measures of general state and trait anxiety (STAI-X1 and STAI-X2) and depressive symptoms (BDI) were included as covariates (see Table 6). Significant unique contributions of the two separate RSFC patterns to the total mediation effect (i.e., ab_1 and ab_2) were not delimitable, but became so when including general trait anxiety or depressive symptoms (here only ab_2) as covariate. No significant difference between the effects of the two mediators (ab_1 vs. ab_2) was found in any of the analyses.

Discussion

In the present study, we successfully applied laughter as social threat to identify non-state-dependent cerebral markers of biased social perception in SA. To our knowledge, this is the first neuroimaging study demonstrating the neuronal correlates of SA-associated cognitive biases in the resting

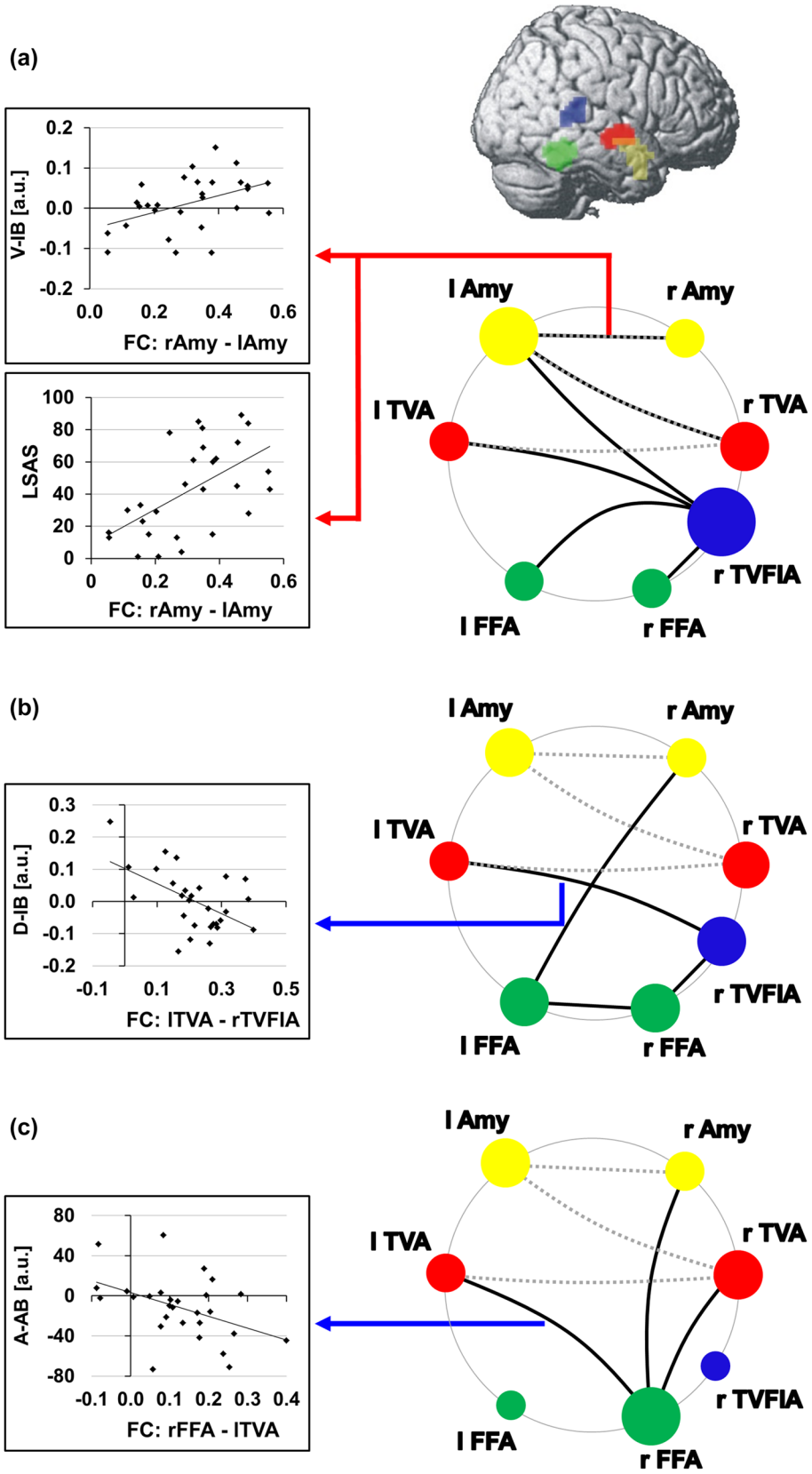

Fig. 5 RSFC correlates of the laughter perception-associated cognitive biases. The regions of interest [bilateral TVA (red), the bilateral FFA (green), the right TVFIA (blue) and the bilateral amygdala (yellow)] are rendered onto the lateral view of a standard brain. The small world diagrams depict the associations of SA severity, the three observed cognitive biases [i.e., **a** laughter valence-related interpretation bias (V-IB), **b** laughter dominance-related interpretation bias (D-IB) and **c** laughter arousal-related attention bias (A-AB)] and the resting state connectivity between the a priori ROIs. Black lines symbolize associations between RSFC and the respective cognitive bias while grey dotted lines represent associations between SA severity and RSFC. Black/grey dotted lines indicate connections where RSFC correlated with SA severity as well as the cognitive bias. *Amy* amygdala. All depicted associations are significant with $p(\mathrm{FDR}) < 0.05$, two-tailed. The dot sizes of the network nodes reflect the number of connections significantly associated with SA severity or the respective cognitive bias. The scatter plots exemplarily visualize the underlying linear associations of RSFC, SA severity and the respective cognitive bias. *LSAS* Liebowitz Social Anxiety Scale. Connectivity estimates given as *Z* transformed correlation coefficients, and bias estimates given in arbitrary units

Table 2 Linear associations between SA and cerebral resting state connectivity

	Peak coordinate (*x y z*)	T-score (peak voxel)	Cluster size (*vx*)
Positive relationship			
Seed: right FFA			
L + R lingual gyri/L inferior and middle occipital gyri/L fusiform gyrus/L + R calcarine gyri	− 3 − 78 − 6	5.9	658*
R + L cuneus/R superior occipital gyrus	6 − 87 33	4.6	328*
Seed: left FFA			
R inferior and middle occipital gyri/R fusiform gyrus/R inferior temporal gyrus/R cerebellum	39 − 69 − 6	4.8	137
R + L supplementary motor area/R superior frontal gyrus/R precentral gyrus/L + R middle cingulum	12 6 48	4.7	294*
R postcentral gyrus/R paracentral lobule/R supplementary motor area/R superior parietal gyrus	21 − 39 54	4.2	167
Seed: right TVA			
L middle and superior temporal gyri/L temporal pole/L Rolandic operculum	− 57 3 − 18	5.3	285*
R postcentral and precentral gyri/L Rolandic operculum/R superior temporal gyrus	63 − 6 15	5.0	181
All other seeds	No significant clusters		
Negative relationship			
Any seed	No significant clusters		

Seed to voxel analysis. Results are shown at a threshold of $p < 0.005$, uncorrected, at voxel-level; cluster significance was assessed using FDR correction ($p < 0.05$) for multiple comparisons across the whole brain. Clusters surviving additional Bonferroni correction for the number of seed ROIs (7) and directions of association (2), i.e., pFDR < 0.0036 are marked with an asterisk. Only clusters significant with pFDR < 0.05 at cluster level are reported. Voxel size: 3 × 3 × 3 mm^3

R right, *L* left

Table 3 Linear associations between the influence of laughter valence on face ratings and cerebral resting state connectivity

	Peak coordinate (*x y z*)	*T* score (peak voxel)	Cluster size (*vx*)
Positive relationship			
Seed: right TVFIA			
L + R calcarine gyri/L lingual gyrus/L + R cuneus/L superior and middle occipital gyri/R precuneus	− 18 − 81 12	4.1	207
Seed: left amygdala			
L inferior and middle temporal gyri/L fusiform and parahippocampal gyri	− 39 − 36 − 15	5.6	303*
All other seeds	No significant clusters		
Negative relationship			
Any seed	No significant clusters		

Seed to voxel analysis. Results are shown at a threshold of $p < 0.005$, uncorrected, at voxel-level; cluster significance was assessed using FDR correction ($p < 0.05$) for multiple comparisons across the whole brain. Clusters surviving additional Bonferroni correction for the number of seed ROIs (7) and directions of association (2), i.e., pFDR < 0.0036 are marked with an asterisk. Only clusters significant with pFDR < 0.05 at cluster level are reported. Voxel size: 3 × 3 × 3 mm^3

R right, *L* left

human brain. This is of particular importance as such cognitive biases have been assumed to be clinically and causally relevant in SA (Clark and Wells 1995; Rapee and Heimberg 1997). The fact that the informative RSFC patterns correlate with the laughter-induced biases across the time lag of 1 month could be interpreted as supporting the notion that the observed connectivity patterns reflect a sustained cerebral disposition for biased perception during the confrontation with social threat.

The dimensional emotional approach (Wundt 1905) in the behavioral assessment enabled the identification of several components of altered social perception associated with SA

Table 4 Linear associations between the influence of laughter dominance on face ratings and cerebral resting state connectivity

	Peak coordinate (*x y z*)	*T* score (peak voxel)	Cluster size (*vx*)
Positive relationship			
Any seed	No significant clusters		
Negative relationship			
Seed: right FFA			
L inferior temporal gyrus/L fusiform gyrus/L inferior occipital gyrus/L lingual gyrus	−45 −42 −21	5.1	248
Seed: right TVA			
L middle and superior frontal gyri/L inferior frontal gyrus, pars triangularis	−24 45 30	5.0	209
Seed: right TVFIA			
R + L lingual gyri/L + R calcarine gyri	18 −60 −3	5.0	308*
L middle occipital gyrus/L angular gyrus/L middle temporal gyrus	−48 −72 15	4.4	282*
L superior and inferior parietal gyri/L precuneus	−18 −78 51	4.3	133
L + R superior frontal gyri partes mediales/R + L medial frontal gyri, partes orbitales/L + R anterior cingulum	−6 54 0	4.2	153
L hippocampus/L middle, inferior and superior temporal gyri	−33 −24 −9	4.1	160
All other seeds	No significant clusters		

Seed to voxel analysis. Results are shown at a threshold of $p < 0.005$, uncorrected, at voxel-level; cluster significance was assessed using FDR correction ($p < 0.05$) for multiple comparisons across the whole brain. Clusters surviving additional Bonferroni correction for the number of seed ROIs (7) and directions of association (2), i.e., pFDR < 0.0036 are marked with an asterisk. Only clusters significant with pFDR < 0.05 at cluster level are reported. Voxel size: 3 × 3 × 3 mm^3

R right, *L* left

in form of valence- and dominance-related interpretation biases and an arousal-related attention bias which, in the first instance, extends findings of laughter-induced cognitive biases (Kreifelts et al. 2014; Ritter et al. 2015) into the domain of contextual, implicit threat processing. Strikingly, all three bias types correlated with patterns of increased RSFC of the amygdala, TVA, FFA and TVFIA. This uniformity suggests that the different bias types may be driven by a common source in the RSFC of the cerebral emotion processing as well as the sensory face and voice perception systems. The positive correlation between RSFC and perception biases, then, may indicate that the increased coherence of neural activity among these regions as well as between these regions and other regions implicated in the processing of faces and other visual cues, in self-processing and in motor functions (see Tables 3, 4, 5) reflects the cerebral correlate of the disposition to exhibit increased sensitivity to negative valence, high dominance and high arousal of contextual signals of social threat in face-to-face communication. While all three biases were associated with SA severity at the behavioral level, a concurrent relationship between SA and the bias-associated RSFC patterns could be ascertained exclusively for the V-IB and the connections between the bilateral amygdalae and between the left amygdala and the right TVA. Thus, these connectivity patterns link SA and behavior in a non-state-dependent fashion across a longer stretch of time potentially dovetailing with the concept of a cerebral trait marker. This notion is further substantiated by the formal mediation of the influence of SA on biased social perception through these connectivity patterns even when accounting for measures of general anxiety and depressive symptoms. The amygdala centricity of the marker patterns fits in well with frequent findings of altered amygdalar RSFC in SA (reviewed in Kim and Yoon 2018) as well as with increased social threat-related amygdala activation (reviewed in Brühl et al. 2014; Miskovic and Schmidt 2012).

Following, we will discuss the separate behavioral and cerebral findings in more detail.

The dimensional perspective on biased perception in SA

In contrast to the common approach of measuring cognitive biases with categorically distinct stimuli (e.g., angry vs. neutral expressions, for reviews see Machado-de-Sousa et al. 2010; Staugaard 2010), the employment of a multidimensional threat continuum using Wundt's (1905) dimensional approach to the assessment of emotions affords an equally multi-faceted assessment of cognitive biases in SA. Accordingly, the complimentary contributions of valence, arousal and dominance to biased perception can be separately evaluated. While the interpretation bias on the valence axis is in line with negative interpretation biases during the processing of differently valenced if categorically distinct

Table 5 Linear associations between the influence of laughter arousal on face rating response times and cerebral resting state connectivity

	Peak coordinate (*x y z*)	*T* score (peak voxel)	Cluster size (*vx*)
Positive relationship			
Seed: right FFA			
L inferior and superior parietal gyri/L postcentral gyrus	−36 −48 48	4.5	161
Seed: left amygdala			
L + R precuneus/L + R cuneus/L + R calcarine gyrus/L posterior cingulum	12 −51 15	5.0	268*
Seed: right amygdala			
R inferior parietal gyrus/R angular gyrus/R supramarginal gyrus	48 −54 45	5.1	197
All other seeds	No significant clusters		
Negative relationship			
Seed: left FFA			
R middle, superior and inferior occipital gyri/R cuneus/R calcarine gyrus	27 −93 −9	5.7	193
L fusiform gyrus/L + R cerebellum incl. vermis/L + R lingual gyrus	−33 −51 −21	5.4	473*
Seed: right FFA			
R inferior frontal gyrus partes triangularis, orbitalis and opercularis	54 30 3	5.5	193
L superior and middle temporal gyrus/L angular gyrus/L supramarginal gyrus/L middle and inferior occipital gyrus	−66 −48 18	5.3	200
L inferior frontal gyrus partes triangularis and orbitalis/L temporal pole/L insula/L superior temporal gyrus	−54 27 3	4.6	296
R middle and superior temporal gyri/R angular gyrus/R middle occipital gyrus	51 −69 18	4.4	139
L Rolandic operculum/L insula/L Heschl's gyrus/L superior temporal gyrus	−39 −24 15	4.3	126
L + R superior frontal gyrus pars medialis/R superior frontal gyrus	3 60 27	3.8	131
R superior and middle temporal gyri/R insula/R Heschl's gyrus	51 −12 0	3.8	131
Seed: right TVFIA			
L posterior cingulum/L + R middle cingulum/L precuneus/L angular gyrus/L cuneus/L superior and middle occipital gyri	−9 −42 27	4.7	395*
Seed: left amygdala			
L + R supplementary motor area/L + R paracentral lobule/R postcentral gyrus/L + R precentral gyrus/R middle cingulum/R superior frontal gyrus/L + R precuneus	9 −30 57	4.6	612*
All other seeds	No significant clusters		

Seed to voxel analysis. Results are shown at a threshold of $p < 0.005$, uncorrected, at voxel-level; cluster significance was assessed using FDR correction ($p < 0.05$) for multiple comparisons across the whole brain. Clusters surviving additional Bonferroni correction for the number of seed ROIs (7) and directions of association (2), i.e., pFDR < 0.0036 are marked with an asterisk. Only clusters significant with pFDR < 0.05 at cluster level are reported. Voxel size: 3 × 3 × 3 mm^3

R right, *L* left

face (Machado-de-Sousa et al. 2010) and voice (Quadflieg et al. 2007) cues, the concurrent interpretation bias on the dominance axis has not been reported before but fits in well with the concept that SA derives from an ancient dominance/submissiveness system subserving social hierarchy (Öhman 1986; Trower and Gilbert 1989). In contrast to laughter valence and dominance which were not reflected in the response time patterns, the opposite was true for laughter arousal. While laughter valence and dominance were imprinted on the face valence ratings, laughter arousal had an increasingly accelerating effect on the participants' responses with increasing SA. This result forms an interesting contrast to research where social threat signals were used as distractors leading to slowed responses in emotional Stroop tasks (Banos et al. 2008; Boehme et al. 2015). One possible explanation for this divergence might be that the target stimuli and unattended stimuli in the present study, in contrast to the emotional Stroop task, were similar enough for high arousal laughter to retrospectively evoke the impression of potential social threat in the neutral target face and lead to quickened responses with increasing SA.

Cerebral correlates of the social perception biases

In contrast to the uniform correlation of the SA-associated laughter perception biases with increased RSFC, the spatial pattern of significant correlations was quite distinctive between the different biases.

Table 6 The influence of SA (*X*) on the laughter valence bias (*Y*) (i.e., more negative face ratings in the context of negative laughter) was mediated through cerebral RSFC patterns (*M*) of the left amygdala

Control variable		$X \rightarrow Y$					$X \rightarrow M$		$M \rightarrow Y$	
		Total effect	Direct effect	Indirect effects						
		c	c'	ab_{TOTAL}	ab_1	ab_2	a_1	a_2	b_1	b_2
None	Beta	0.001	0.0002	0.0008	0.0004	0.0003	0.0029	0.0014	0.145	0.250
	(SE/95% CI)	(0.0004)	(0.0005)	(0.0001–0.0017)	(−0.0001 to 0.0012)	(0.0000 to 0.0012)	(0.0008)	(0.0006)	(0.097)	(0.141)
STAI-X1	Beta	0.0008	−0.0001	0.0009	0.0005	0.0003	0.0034	0.0014	0.153	0.248
	(SE/95% CI)	(0.0006)	(0.0007)	(0.0001–0.0021)	(−0.0001 to 0.0015)	(−0.0001 to 0.0014)	(0.0011)	(0.0008)	(0.099)	(0.143)
STAI-X2	Beta	0.0006	−0.0014	0.0021	0.0007	0.0014	0.0037	0.0029	0.192	0.471
	(SE/95% CI)	(0.0006)	(0.0007)	(0.0011–0.0034)	(0.0002 to 0.0015)	(0.0005 to 0.0024)	(0.0012)	(0.0007)	(0.087)	(0.147)
BDI	Beta	0.0012	−0.0001	0.0014	0.0007	0.0007	0.0041	0.0023	0.159	0.306
	(SE/95% CI)	(0.0006)	(0.0007)	(0.0003–0.0029)	(−0.0002 to 0.0018)	(0.0001 to 0.0019)	(0.0011)	(0.0007)	(0.096)	(0.143)

Mediation analysis: *X* = independent variable, *Y* = dependent variable, *M* = mediator, *a* = influence of *X* on *M*, *b* = influence of *M* on *Y* controlling for *X*, *c* = total effect of *X* on *Y*, *c'* = direct effect of *X* on *Y*, *ab* = indirect effect of *X* on *Y* through *M*. M_1 = RSFC between left amygdala and right amygdala, M_2 = RSFC between left amygdala and right TVA. *a*, *b* and *ab* are numbered respectively. ab_{TOTAL} = total indirect effect of *X* on *Y* through M_1 and M_2. *SE* standard error. 95% CI refer to the employed bootstrapping approach to estimate indirect effects (see "Materials and methods")

At the ROI level, the left amygdala and foremost the right TVFIA were the central nodes around which the valence bias-associated RSFC connections to all other ROIs of the cerebral voice-, face- and emotion-processing systems were clustered. Especially, the central position of the right TVFIA RSFC patterns appears plausible keeping in mind that the bias temporally predicted by these patterns was induced by bimodal face-voice-cues the sensory information of which is integrated in this area (Ethofer et al. 2013; Kreifelts et al. 2007, 2009; Pourtois et al. 2005; Robins et al. 2009). The RSFC patterns associated with the D-IB, in contrast, were less numerous and more evenly distributed among the ROIs, however, with a spatial overlap with the valence bias-related RSFC patterns in the connections between the right TVFIA and the left TVA as well as the right FFA. This coincidence highlights the potential particular importance of the resting state interplay between the TVFIA and the respective unimodal voice- and face-sensitive cortices as non-state-dependent cerebral markers of interpretation biases during social perception. The RSFC patterns associated with the A-AB were non-overlapping with those predictive of the interpretation biases and did not include the TVFIA, potentially implying the particular significance of the interplay between this functional module and earlier sensory voice and face processing units for the manifestation of an interpretation bias during the contextual perception of social threat signals which would be in good agreement with current neurobiological models of multimodal affective information processing (e.g., Brück et al. 2011).

Moreover, it is worthwhile noting that amygdalar connectivity patterns were part of the cerebral resting state representation of each of the three biases as an indicator that the preparedness to exhibit these perception biases is not only represented in the sensory face-voice-processing systems alone (e.g., reflecting sensory tuning) but also in their connections to the emotion-processing network.

At the whole brain level, our study identified a number of resting state correlates of social perception biases outside the primary focus of the connectivity between the predefined ROI. Increased RSFC between the predefined nodes of the face-voice- and emotion-processing network and various areas in the visual associative cortex outside the FFA, in correlation with the interpretation biases, indicates that the non-state-dependent cerebral bias markers are not restricted to face-preferential regions of the visual cortex but obviously include other aspects of visual processing as well. The precise functionality of these connectivity patterns outside the primary ROI is scarcely deducible within the framework of this study and considering the lack of previous comparable studies, one exception being the association of the dominance bias and increased RSFC between the right TVFIA, the left posterior aspects of the STS and the bilateral lingual gyri which taken together

with increased RSFC between the right TVFIA and the right FFA fit in well with a previous fMRI study reporting processing correlates of social dominance communicated via facial cues in the posterior superior temporal, lingual and fusiform gyri (Chiao et al. 2008). Thus, the RSFC patterns between these regions and the TVFIA, as part of the whole dominance bias-related RSFC pattern, may well reflect that component of the disposition to exhibit increased sensitivity to high laughter dominance based on face cues.

The arousal-related bias, finally, paralleled the other two bias types in its association with RSFC patterns of the visual associative cortex outside the FFA but was the only bias for which predictive RSFC patterns were detected in connections outside the amygdala and sensory cortices related to audiovisual perception. While it appears conceptually well comprehensible that the individual influence of laughter arousal on response times should be reflected in the RSFC between the amygdala and supplementary motor cortices, the reflection of the very same bias in the RSFC between the right TVFIA and the precuneus/posterior cingulate cortex (PCC) warrants a more detailed discussion. It might be hypothesized that this cerebral bias correlate mirrors the individual propensity to relate emotional information extracted from the audiovisual threat stimulus (Brück et al. 2011) to concepts of the self and self-processing (Northoff et al. 2006) as predictor for the occurrence of the bias during threat confrontation. This interpretation then dovetails with a considerable body of evidence for permanently biased self-processing (Clark and McManus 2002) and alterations in precuneus RSFC in SA (Liu et al. 2015).

Remarkably, none of the social perception biases was reflected in the RSFC patterns of the lateral and dorsolateral prefrontal cortex where the cerebral correlates of such biases and their modification through emotion regulation were observed during confrontation with social threat in healthy participants (Browning et al. 2010) and in SA (Kreifelts et al. 2014, 2017). This disparity very clearly supports the notion that the informative RSFC patterns reported here do not represent the cerebral correlates of biased social perception in SA per se but of the SA-related predisposition to exhibit perception biases when confronted with social threat. The negative finding for the lateral and dorsolateral aspects of the prefrontal cortex also appears to dovetail with previous connectivity studies demonstrating that emotion regulatory effects of the prefrontal cortex on the amygdala were rather mediated by the medial orbitofrontal cortex than the DLPFC (Sladky et al. 2015) and that such connectivity patterns were strongly influenced by task and cognitive load (Minkova et al. 2017) which again might explain the negative finding also for this region in our study and strongly advocate the inclusion of these factors in the assessment of cerebral connectivity patterns.

Implications for future research

Keeping in mind the assumption that biased perception of potential social threat signals is causal in the perpetuation of SA (Amir et al. 2009; Amir and Taylor 2012; Beard and Amir 2008; Clark and Wells 1995; Rapee and Heimberg 1997) and asking the question if the cerebral markers described in this study are in any way causal to the occurrence of biased social perception in SA, two interesting avenues for prospective research projects can be envisaged. The direction of the first would be towards a better understanding of SA therapy, and of the second towards the potential development of better SA therapies. While some progress has been made in the elucidation of the neural underpinnings of treatment interventions in SA [e.g., cognitive behavioral therapy (Goldin et al. 2013, 2014; Yuan et al. 2016, 2018)] this knowledge could be considerably extended taking into account the effects of SA treatment on the cerebral markers of social perception biases. From the reverse perspective, one may ask how the modulation of the cerebral marker patterns, for example, by real-time fMRI connectivity feedback (Watanabe et al. 2017) might affect, potentially reduce, perception biases in SA. This would provide a means which could be used to directly test the causal significance of the cerebral marker patterns for biased social perception, and could also be evaluated for its potential to reduce SA through the non-invasive modulation of cerebral resting state activity.

Limitations

The generalizability of our findings could be limited by the relatively young study population even if the highest prevalence rates of pronounced SA (Jacobi et al. 2014) coincide well with the age range of the present study. Despite the fact that almost half of the study population exhibited clinically relevant SA, future clinically focused studies should verify that the results of our dimensional approach are directly transferable to the dichotomous distinction between individuals with SAD and the healthy population, ideally with larger sample sizes. Finally, the novelty of our experimental approach and the lack of previous research on resting state markers of biased social perception in SA impose certain restrictions on the interpretation of the observed connectivity patterns beyond their established non-state-dependent relationship with biased social perception. Thus, all further conceptions on the potential underpinnings of these patterns presented here need to be treated as completely novel and consequently tentative requiring verification through future research.

Conclusion

Using laughter as social threat, this study succeeded in delineating behaviorally relevant non-state-dependent cerebral markers of SA. Based on a dimensional approach, different components of biased social perception were identified. While the arousal level of the threat signal was driving a SA-associated attention bias, the observed interpretation bias was driven by the valence and dominance imbued in the laughter signal. These different correlates of biased social perception were distinct in their cerebral representation among the amygdalae and central nodes of the cerebral voice and face processing system with only moderate overlaps between the interpretation bias components attributable to laughter valence and dominance. Critically, the RSFC patterns of the left amygdala stood out in a particular manner exhibiting all necessary characteristics of a cerebral mediator of the influence of SA on the valence-associated social perception bias.

Beyond elucidating the cerebral underpinnings of the assumedly causal relationship between SA and social perception biases, the relevance of these findings is further extended through the time lag between the RSFC and behavioral measurements which, in contrast to previous neuroimaging studies, is adjusted to the concept of SA as a permanent anxiety rather than a situational phobic fear.

Acknowledgements This work was supported by grants of the Fortüne-Program of the University of Tübingen (fortüne 1997-0-0, and fortüne 2140-0-0).

References

Amir N, Taylor CT (2012) Interpretation training in individuals with generalized social anxiety disorder: a randomized controlled trial. J Consult Clin Psychol 80(3):497–511. https://doi.org/10.1037/a0026928

Amir N, Beard C, Taylor CT, Klumpp H, Elias J, Burns M, Chen X (2009) Attention training in individuals with generalized social phobia: a randomized controlled trial. J Consult Clin Psychol 77(5):961–973

Banos RM, Quero S, Botella C (2008) Detection and distraction effects for threatening information in social phobia and change after treatment. Depress Anxiety 25(1):55–63. https://doi.org/10.1002/da.20269

Beard C, Amir N (2008) A multi-session interpretation modification program: changes in interpretation and social anxiety symptoms. Behav Res Ther 46(10):1135–1141. https://doi.org/10.1016/j.brat.2008.05.012

Belin P, Zatorre RJ, Lafaille P, Ahad P, Pike B (2000) Voice-selective areas in human auditory cortex. Nature 403(6767):309–312

Boehme S, Ritter V, Tefikow S, Stangier U, Strauss B, Miltner WH, Straube T (2015) Neural correlates of emotional interference in social anxiety disorder. PLoS One 10(6):e0128608. https://doi.org/10.1371/journal.pone.0128608

Browning M, Holmes EA, Murphy SE, Goodwin GM, Harmer CJ (2010) Lateral prefrontal cortex mediates the cognitive modification of attentional bias. Biol Psychiatry 67(10):919–925

Brück C, Kreifelts B, Wildgruber D (2011) Emotional voices in context: a neurobiological model of multimodal affective information processing. Phys Life Rev 8(4):383–403

Brühl AB, Delsignore A, Komossa K, Weidt S (2014) Neuroimaging in social anxiety disorder-a meta-analytic review resulting in a new neurofunctional model. Neurosci Biobehav Rev 47:260–280

Chiao JY, Adams RB, Tse PU, Lowenthal L, Richeson JA, Ambady N (2008) Knowing who's boss: fMRI and ERP investigations of social dominance perception. Group Process Intergroup Relat GPIR 11(2):201–214. https://doi.org/10.1177/1368430207088038

Clark DM, McManus F (2002) Information processing in social phobia. Biol Psychiatry 51(1):92–100

Clark DM, Wells A (1995) A cognitive model of social phobia. In: Heimberg RG, Liebowitz MR, Hope DA, Schneier FR (eds) Social phobia: diagnosis, assessment, and treatment. Guilford Press, New York, pp 69–93

Davila Ross M, Owren MJ, Zimmermann E (2009) Reconstructing the evolution of laughter in great apes and humans. Curr Biol 19(13):1106–1111

Eibl-Eibesfeldt I (1970) Ethology: the biology of behavior. Holt, Rinehart and Winston, New York

Epstein R, Harris A, Stanley D, Kanwisher N (1999) The parahippocampal place area: recognition, navigation, or encoding? Neuron 23(1):115–125

Ethofer T, Bretscher J, Wiethoff S, Bisch J, Schlipf S, Wildgruber D, Kreifelts B (2013) Functional responses and structural connections of cortical areas for processing faces and voices in the superior temporal sulcus. NeuroImage 76C:45–56

Gilboa-Schechtman E, Foa EB, Amir N (1999) Attentional biases for facial expressions in social phobia: the effects of target and distractor in "face-in-the-crowd" task. Cogn Emot 13:305–318

Goldin PR, Ziv M, Jazaieri H, Hahn K, Heimberg R, Gross JJ (2013) Impact of cognitive behavioral therapy for social anxiety disorder on the neural dynamics of cognitive reappraisal of negative self-beliefs: randomized clinical trial. JAMA Psychiatry 70(10):1048–1056. https://doi.org/10.1001/jamapsychiatry.2013.234

Goldin PR, Ziv M, Jazaieri H, Weeks J, Heimberg RG, Gross JJ (2014) Impact of cognitive-behavioral therapy for social anxiety disorder on the neural bases of emotional reactivity to and regulation of social evaluation. Behav Res Ther 62:97–106. https://doi.org/10.1016/j.brat.2014.08.005

Hautzinger M (1991) The Beck Depression Inventory in clinical practice. Der Nervenarzt 62(11):689–696

Havranek MM, Volkart F, Bolliger B, Roos S, Buschner M, Mansour R, Chmielewski T, Gaudlitz K, Hattenschwiler J, Seifritz E, Ruch W (2017) The fear of being laughed at as additional diagnostic criterion in social anxiety disorder and avoidant personality disorder? PLoS One 12(11):e0188024. https://doi.org/10.1371/journal.pone.0188024

Jacobi F, Hofler M, Strehle J, Mack S, Gerschler A, Scholl L, Busch MA, Maske U, Hapke U, Gaebel W, Maier W, Wagner M, Zielasek J, Wittchen HU (2014) Mental disorders in the general population: study on the health of adults in Germany and the additional module mental health (DEGS1-MH). Der Nervenarzt 85(1):77–87. https://doi.org/10.1007/s00115-013-3961-y

Kanwisher N, McDermott J, Chun MM (1997) The fusiform face area: a module in human extrastriate cortex specialized for face perception. J Neurosci 17(11):4302–4311

Kim YK, Yoon HK (2018) Common and distinct brain networks underlying panic and social anxiety disorders. Prog Neuro-psychopharmacol Biol Psychiatry 80(Pt B):115–122. https://doi.org/10.1016/j.pnpbp.2017.06.017

Kreifelts B, Ethofer T, Grodd W, Erb M, Wildgruber D (2007) Audiovisual integration of emotional signals in voice and face: an event-related fMRI study. NeuroImage 37(4):1445–1456

Kreifelts B, Ethofer T, Shiozawa T, Grodd W, Wildgruber D (2009) Cerebral representation of non-verbal emotional perception: fMRI reveals audiovisual integration area between voice- and face-sensitive regions in the superior temporal sulcus. Neuropsychologia 47(14):3059–3066

Kreifelts B, Ethofer T, Huberle E, Grodd W, Wildgruber D (2010) Association of trait emotional intelligence and individual fMRI-activation patterns during the perception of social signals from voice and face. Humn Brain Mapp 31(7):979–991

Kreifelts B, Jacob H, Bruck C, Erb M, Ethofer T, Wildgruber D (2013) Non-verbal emotion communication training induces specific changes in brain function and structure. Front Hum Neurosci 7:648

Kreifelts B, Brück C, Ritter J, Ethofer T, Domin M, Lotze M, Jacob H, Schlipf S, Wildgruber D (2014) They are laughing at me: cerebral mediation of cognitive biases in social anxiety. PLoS One 9(6):e99815

Kreifelts B, Brück C, Ethofer T, Ritter J, Weigel L, Erb M, Wildgruber D (2017) Prefrontal mediation of emotion regulation in social anxiety disorder during laughter perception. Neuropsychologia 96:175–183. https://doi.org/10.1016/j.neuropsychologia.2017.01.016

Laux L, Glanzmann P, Schaffner P, Spielberger CD (1981) Das State-Trait-Angstinventar. Beltz, Weinheim

Lehrl S (2005) Mehrfachwahl-Wortschatz-Intelligenztest MWT-B, 5th edn. Spitta, Balingen

Lipsitz JD, Schneier FR (2000) Social phobia. Epidemiology and cost of illness. Pharmacoeconomics 18(1):23–32

Liu F, Zhu C, Wang Y, Guo W, Li M, Wang W, Long Z, Meng Y, Cui Q, Zeng L, Gong Q, Zhang W, Chen H (2015) Disrupted cortical hubs in functional brain networks in social anxiety disorder. Clin Neurophysiol 126(9):1711–1716. https://doi.org/10.1016/j.clinph.2014.11.014

Machado-de-Sousa JP, Arrais KC, Alves NT, Chagas MH, de Meneses-Gaya C, Crippa JA, Hallak JE (2010) Facial affect processing in social anxiety: tasks and stimuli. J Neurosci Methods 193(1):1–6

Mendlowicz MV, Stein MB (2000) Quality of life in individuals with anxiety disorders. Am J Psychiatry 157(5):669–682

Minkova L, Sladky R, Kranz GS, Woletz M, Geissberger N, Kraus C, Lanzenberger R, Windischberger C (2017) Task-dependent modulation of amygdala connectivity in social anxiety disorder. Psychiatry Res Neuroimaging 262:39–46. https://doi.org/10.1016/j.pscychresns.2016.12.016

Miskovic V, Schmidt LA (2012) Social fearfulness in the human brain. Neurosci Biobehav Rev 36(1):459–478

Mogg K, Bradley BP (2002) Selective orienting of attention to masked threat faces in social anxiety. Behav Res Ther 40(12):1403–1414

Northoff G, Heinzel A, de Greck M, Bermpohl F, Dobrowolny H, Panksepp J (2006) Self-referential processing in our brain—a meta-analysis of imaging studies on the self. NeuroImage 31(1):440–457. https://doi.org/10.1016/j.neuroimage.2005.12.002

Öhman A (1986) Face the beast and fear the face: animal and social fears as prototypes for evolutionary analyses of emotion. Psychophysiology 23(2):123–145

Oldfield RC (1971) The assessment and analysis of handedness: the Edinburgh inventory. Neuropsychologia 9(1):97–113

Pernet CR, McAleer P, Latinus M, Gorgolewski KJ, Charest I, Bestelmeyer PE, Watson RH, Fleming D, Crabbe F, Valdes-Sosa M, Belin P (2015) The human voice areas: spatial organization and inter-individual variability in temporal and extra-temporal cortices. NeuroImage 119:164–174

Pourtois G, de Gelder B, Bol A, Crommelinck M (2005) Perception of facial expressions and voices and of their combination in the human brain. Cortex 41(1):49–59

Preacher KJ, Hayes AF (2008) Asymptotic and resampling strategies for assessing and comparing indirect effects in multiple mediator models. Behav Res Methods 40(3):879–891

Provine RR (2013) Laughing, grooming, and pub science. Trends Cogn Sci 17(1):9–10

Quadflieg S, Wendt B, Mohr A, Miltner WH, Straube T (2007) Recognition and evaluation of emotional prosody in individuals with generalized social phobia: a pilot study. Behav Res Ther 45(12):3096–3103

Rapee RM, Heimberg RG (1997) A cognitive-behavioral model of anxiety in social phobia. Behav Res Ther 35(8):741–756

Ritter J, Brück C, Jacob H, Wildgruber D, Kreifelts B (2015) Laughter perception in social anxiety. J Psychiatr Res 60C:178–184

Robins DL, Hunyadi E, Schultz RT (2009) Superior temporal activation in response to dynamic audio-visual emotional cues. Brain Cogn 69(2):269–278

Sladky R, Hoflich A, Kublbock M, Kraus C, Baldinger P, Moser E, Lanzenberger R, Windischberger C (2015) Disrupted effective connectivity between the amygdala and orbitofrontal cortex in social anxiety disorder during emotion discrimination revealed by dynamic causal modeling for FMRI. Cereb Cortex 25(4):895–903. https://doi.org/10.1093/cercor/bht279

Stangier U, Heidenreich T (2003) Die Liebowitz Soziale Angst-Skala (LSAS). Collegium Internationale Psychiatriae Scalarum - Internationale Skalen für Psychiatrie. Hogrefe, Göttingen

Staugaard SR (2010) Threatening faces and social anxiety: a literature review. Clin Psychol Rev 30(6):669–690

Stein DJ, Ruscio AM, Lee S, Petukhova M, Alonso J, Andrade LH, Benjet C, Bromet E, Demyttenaere K, Florescu S, de Girolamo G, de Graaf R, Gureje O, He Y, Hinkov H, Hu C, Iwata N, Karam EG, Lepine JP, Matschinger H, Oakley Browne M, Posada-Villa J, Sagar R, Williams DR, Kessler RC (2010) Subtyping social anxiety disorder in developed and developing countries. Depress Anxiety 27(4):390–403

Szameitat DP, Alter K, Szameitat AJ, Darwin CJ, Wildgruber D, Dietrich S, Sterr A (2009) Differentiation of emotions in laughter at the behavioral level. Emotion 9(3):397–405

Trower P, Gilbert P (1989) New theoretical conceptions of social anxiety and social phobia. Clin Psychol Rev 9(1):19–35. https://doi.org/10.1016/0272-7358(89)90044-5

Tzourio-Mazoyer N, Landeau B, Papathanassiou D, Crivello F, Etard O, Delcroix N, Mazoyer B, Joliot M (2002) Automated anatomical labeling of activations in SPM using a macroscopic anatomical parcellation of the MNI MRI single-subject brain. NeuroImage 15(1):273–289

Watanabe T, Sasaki Y, Shibata K, Kawato M (2017) Advances in fMRI real-time neurofeedback. Trends Cogn Sci 21(12):997–1010. https://doi.org/10.1016/j.tics.2017.09.010

Werner S, Noppeney U (2010) Superadditive responses in superior temporal sulcus predict audiovisual benefits in object categorization. Cereb Cortex 20(8):1829–1842

Whitfield-Gabrieli S, Nieto-Castanon A (2012) Conn: a functional connectivity toolbox for correlated and anticorrelated brain networks. Brain Connect 2(3):125–141. https://doi.org/10.1089/brain.2012.0073

Wittchen HU, Zaudig M, Fydrich T (1997) Strukturiertes Klinisches Interview für DSM-IV. Hogrefe, Göttingen

Worsley K, Marrett S, Neelin P, Vandal AC, Friston KJ, Evans A (1996) A unified statistical approach for determining significant signals in images of cerebral activation. Hum Brain Mapp 4(1):74–90

Wundt W (1905) Grundzüge der physiologischen Psychologie, 5th edn. Engelmann, Leipzig

Yuan M, Zhu H, Qiu C, Meng Y, Zhang Y, Shang J, Nie X, Ren Z, Gong Q, Zhang W, Lui S (2016) Group cognitive behavioral therapy modulates the resting-state functional connectivity of amygdala-related network in patients with generalized social anxiety disorder. BMC Psychiatry 16:198. https://doi.org/10.1186/s12888-016-0904-8

Yuan M, Zhu H, Qiu C, Meng Y, Zhang Y, Ren Z, Li Y, Yuan C, Gao M, Lui S, Gong Q, Zhang W (2018) Altered regional and integrated resting-state brain activity in general social anxiety disorder patients before and after group cognitive behavior therapy. Psychiatry Res 272:30–37. https://doi.org/10.1016/j.pscychresns.2017.12.004